Applied Physics A (2018) 124:294
https://doi.org/10.1007/s00339-018-1710-6

Applied Physics A
Materials Science & Processing

Angle-dependent tribological properties of AlCrN coatings with microtextures induced by nanosecond laser under dry friction

Youqiang Xing[1] · Jianxin Deng[2] · Peng Gao[2] · Juntao Gao[1] · Ze Wu[1]

Received: 8 October 2017 / Accepted: 27 February 2018 / Published online: 12 March 2018

Abstract
Microtextures with different groove inclinations are fabricated on the AlCrN-coated surface by a nanosecond laser, and the tribological properties of the textured AlCrN samples sliding against AISI 1045 steel balls are investigated by reciprocating sliding friction tests under dry conditions. Results show that the microtextures can effectively improve the tribological properties of the AlCrN surface compared with the smooth surface. Meanwhile, the angle between the groove inclination and sliding direction has an important influence on the friction and wear properties. The textured sample with the small groove inclination may be beneficial to reducing the friction and adhesions, and the TC-0° sample exhibits the lowest friction coefficient and adhesions of the worn surface. The wear volume of the ball sliding against the TC-0° sample is smaller compared with the UTC sample and the sliding against the TC-45° and TC-90° samples is larger compared with the UTC sample. Furthermore, the mechanisms of the microtextures are discussed.

1 Introduction

Due to the high hardness, high oxidation resistance, and excellent wear resistance, AlCrN coatings are regarded as an excellent candidate to be used for reducing wear and increasing the life, and they are widely used in engineering components and cutting tools [1, 2]. The AlCrN coatings can be used in dry or lubricated conditions; however, the AlCrN coatings still suffer high friction and wear under dry conditions, which limit their applications in engineering. Especially, in dry cutting process, the high friction coefficient occurs at the tool–chip interface of the AlCrN-coated cutting tools when in machining of steel, which reduces the tool life [3, 4]. Recently, texturing of the coated surfaces can be a potential method to reduce the friction and wear and that has been used in cutting tools or tribology communities. For examples, Zhang et al. [5] reported that the TiAlN-coated tools with micro/nanotextures can improve the cutting properties compared with untextured TiAlN-coated tools. Obikawa et al. [6] fabricated four microtextured DLC- and TiN-coated tools, and results showed that suitable surface textures can effectively reduce the friction and wear. Shum et al. [7] demonstrated that the TiAlSiN coatings with the dimpled textures and ion implantation improved the friction and wear performance compared with the untreated-coated surface. Voevodin and Zabinski [8] reported that the dimples as microreservoirs provided friction and wear reduction of TiCN-coated surface compared with the untextured surface in variable solid lubricated conditions. Dumitru et al. [9] used a femtosecond laser to produce the microtextures on TiN- and TiCN-coated surfaces, and the results exhibited that the textured surface showed significantly better tribological performance than untextured coated surface.

In spite of the evidence that the surface textures can improve the tribological performance, considerable experiments demonstrated that the geometry of the textures has an important effect on the friction and wear properties. Dimples and grooves are the most common textures, and the dimples are better to obtain the hydrodynamic effect compared with the grooves under liquid-lubricated conditions [10, 11]. However, the grooves are widely used in cylinder liner [12, 13], and researches show that the grooves exhibit better tribological performance than dimples in many fields [14, 15]. Meanwhile, the angle of the groove inclination and sliding direction has an important influence on the friction and wear properties.

✉ Jianxin Deng
jxdeng@sdu.edu.cn

[1] School of Mechanical Engineering, Southeast University, Nanjing 211189, Jiangsu, People's Republic of China

[2] Key Laboratory of High Efficiency and Clean Mechanical Manufacture of MOE, School of Mechanical Engineering, Shandong University, Jinan 250061, Shandong, People's Republic of China

Pettersson and Jacobson [16] studied that, under starved boundary lubrication conditions, the grooves with an orientation perpendicular to the sliding direction exhibited very low and stable friction and much better wear resistance than the untextured surface, and the surface with grooves along the sliding direction was not able to provide sufficient lubricant within the contact zone. While, the results contradicted to that reported by Hata et al. [17]. Rosenkranz et al. [18] studied the alignment effect between laser-patterned steel surfaces under dry-sliding conditions, and results showed that the grooves perpendicular to the sliding direction showed a lower friction coefficient compared with the parallel configuration. Wang et al. [19] investigated the effect of groove inclination and sliding direction on the tribological properties of stainless steel sliding against Al_2O_3 ceramic ball under lubricated conditions, they reported that the tribological performance depended on the inclination angles of microgrooves, and the grooves perpendicular to the sliding direction exhibited the lowest friction coefficient and wear rate. Yuan et al. [20] studied the orientation effect of grooves on the friction performance under liquid-lubricated conditions, and the results showed that, under a relatively low contact pressure, the grooves that perpendicular to the sliding direction had a better effect on friction reduction than that of parallel orientation; under a relatively high contact pressure, the grooves that parallel to the sliding direction exhibited better friction properties than that of perpendicular orientation. Costa and Hutchings [21] reported that the sample with grooves parallel to the sliding direction showed the best lubricity than the other orientation with the small load and that had the worst lubricity with the high load. Mezghani et al. [22] and Suh et al. [23] studied that the angle of liner crosshatch grooves seemed to be an important parameter to design the grooves for friction reduction by numerical analysis and experimental methods. Even though the surface textures can improve the friction properties, they can also increase the friction in different conditions [24–27]. Based on the above reviews, friction and wear properties of the textured surfaces are sensitive to the groove inclination and experimental conditions, which need to be further investigated.

In this paper, the microtextures are fabricated on AlCrN coatings by a nanosecond laser, the friction, and wear properties of the textured AlCrN surface sliding against AISI 1045 steel ball are studied by reciprocating sliding ball-on-disk tests under dry conditions. The main aim of the investigation is to assess the effect of groove inclination on AlCrN-coated surface for reducing the friction and wear.

2 Experimental details

2.1 Materials and surface texturing

The specimens used for the friction tests are AlCrN-coated carbide disks with the size of 16 mm × 16 mm × 4.5 mm, and the friction mates used are AISI 1045-hardened steel balls with a diameter of 9.525 mm and hardness of 50–60 HRC. The substrate material of the coated disk is YG6-cemented carbide, and the compositions and mechanical properties of the cemented carbide are listed in Table 1. The substrate surfaces are lapped and polished to the roughness Ra less than 0.1 μm, and then, they are cleaned in an ultrasonic bath by alcohol and each for 20 min. After that, they are dried for approximately 10 min in a pre-vacuum dryer. AlCrN coatings are deposited onto the substrate surfaces by a physical vapor deposition method with a high purity of Al and Cr targets. Figure 1 shows the surface micrograph, cross section of the coatings, and the EDX analysis. As shown in the figure, the AlCrN coatings are dense without cracks and pores, and the thickness of the AlCrN coatings is about 3 μm. The composition and properties of the AlCrN coatings are presented in Table 2.

Microtextures with different orientations and spacing are produced on the AlCrN-coated samples by ablation directly with a higher energy absorption of 90–93% using an Nd:YAG laser with a wavelength of 1064 nm and pulse duration of 10 ns (DP-H50, Jinan Xinchu Co., Ltd., China). The AlCrN-coated samples are mounted on a three-dimensional XYZ stage and a single laser beam is focused on the sample surface by a lens with focal length of 63 mm. The incident angle of the laser beam with respect to sample surface is near normal and the preparation process is monitored by a digital microscope focusing on the sample. The experiments are conducted under atmospheric pressure and room temperature with the following processing parameters: power of 12 W, scanning speed of 20 mm/s, frequency of 20 kHz, and pulse overlap of 0.98. The microgrooves are fabricated in an area with the length of 12 mm and width of 12 mm, and the spacing of microgrooves is 300, 400, and 500 μm. The samples with the angles between the groove inclination and sliding direction of 0°, 45°, and 90° are named TC-0°, TC-45°, and TC-90°, respectively, and the untextured

Table 1 Composition and mechanical properties of the cemented carbide substrate

Composition (wt%)	Hardness (HRA)	Density (g/cm^3)	Thermal conductivity (W/(m K))	Elastic modulus (GPa)
WC + 6%Co	91.0	14.8	79.6	640

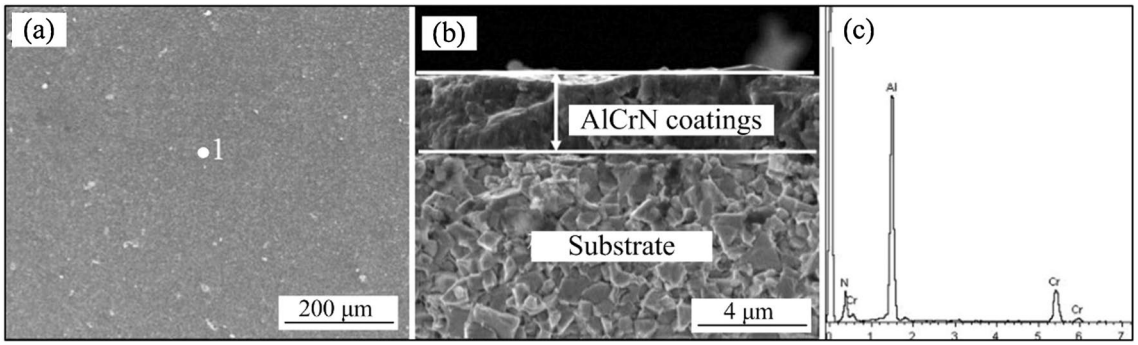

Fig. 1 SEM micrographs of the coated surface (**a**), cross section (**b**), and the EDX analysis of point 1 (**c**)

Table 2 Composition and properties of AlCrN coating

Coating	Elemental composition (at.%)	Coatings thickness (μm)	Hardness (HV)	Critical load (N)
AlCrN	34.6% Al/14.7% Cr/50.7% N	3.0	3200	85.1

samples (named UTC) are used for comparison. The surface topography and profile of the textured samples are measured by an optical microscope with 3D profilometer (VHX-600, Japan).

2.2 Friction and wear test

Reciprocating ball-on-disk friction and wear tests are conducted on a tribometer (UMT-2, USA) in air atmosphere to investigate the angle-dependent tribological properties of AlCrN coatings with microtextures. The lower sample of AlCrN-coated disk is fixed and the upper sample of 1045 steel ball is reciprocating against the lower sample. All tests are carried out with a load of 10 N, sliding speed of 10 mm/s, a stroke of 10 mm, and sliding time of 30 min. Each test is repeated twice. Before the tests, all samples are cleaned with 20 min ultrasonic bath in acetone and alcohol, respectively.

The surface morphologies and profiles of wear tracks after tests are measured by a scanning electron microscope (SEM, QUANTA FEG250, USA) and white light interferometer (WYKO NT9300, USA). Chemical compositions of the samples are detected by an energy-dispersive X-ray spectroscope system (EDX, X-MAX50, UK). The worn morphologies of counter balls are measured by an SEM and optical microscope. The wear volumes of the balls are calculated based on the diameter of the worn scars on the spherical crown measured by an optical microscope [28].

3 Results and discussion

3.1 Morphology of laser-textured surfaces

Figure 2 shows the optical micrographs and schematic diagram of textured AlCrN surface with different groove inclinations at the spacing of 400 μm (TC-0°, TC-45°, and TC-90°). It is observed that the microgrooves are regularly arranged on the AlCrN-coated surface. θ is the angle between the groove inclination and the sliding direction. The three-dimensional surface topography and profile of a single microgroove are measured by an optical microscope and that are shown in Fig. 3. It demonstrates that the width of the groove is about 50 μm and the depth is about 3 μm. Figure 4 shows the SEM images of micro/nanotopographies and the EDX analysis of the groove. It can be seen that the heat-affected zone is formed surrounding the groove due to the interaction between the laser with high-energy density and the coatings (Fig. 4a). The molten materials deposit on the brims and sidewalls of the groove and then condense rapidly, forming the recast layers as can be observed from the enlarged zone A in Fig. 4b, and the molten materials deposit on zone B forming the micro/nanoparticles (Fig. 4c). Meanwhile, the EDX analyses of line CD exhibit lower content of N, Cr, and Al and higher content of C, W, and Co in the groove, which indicates that the substrate is exposed.

3.2 Friction coefficient

Figure 5 shows the friction coefficient of the smooth and textured AlCrN samples with different groove inclinations at the different spacings as a function of increasing sliding time. As shown in this figure, the friction coefficient of the smooth and textured AlCrN coatings is significantly different and the friction curves initially oscillate and then tend to be steady waves. The friction coefficient of the textured AlCrN samples is lower compared with the smooth surface, and the angle between the groove inclination and sliding direction has an important effect on the friction coefficient.

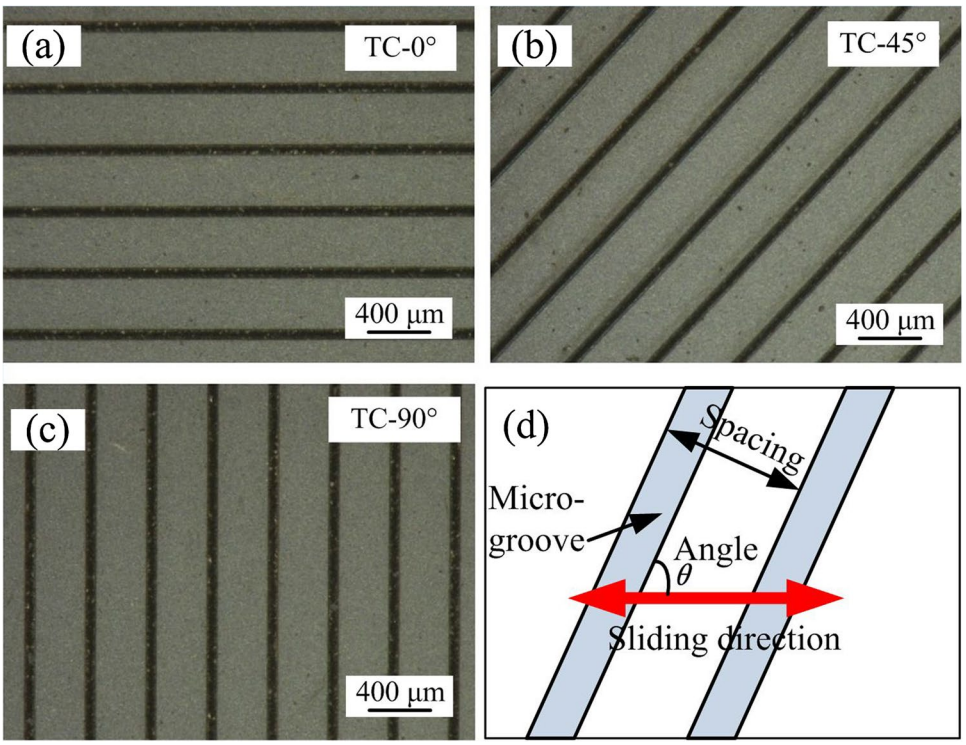

Fig. 2 Optical micrographs of textured AlCrN surface with different groove inclinations. **a** TC-0°, **b** TC-45°, **c** TC-45°, and the schematic diagram of the textured surface (**d**)

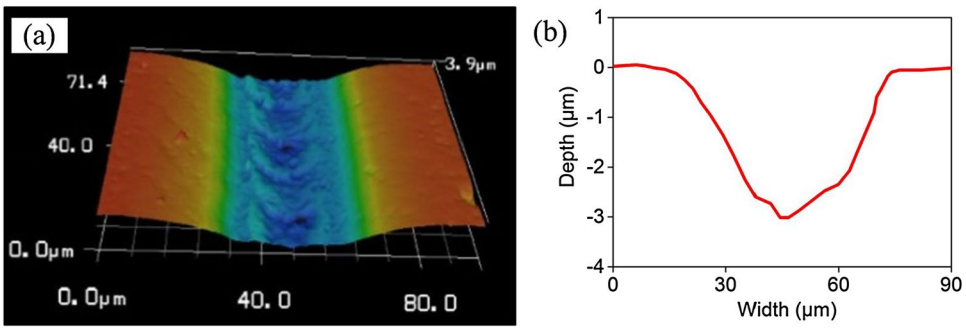

Fig. 3 Three-dimensional surface topography and profile of a single microgroove

It can be clearly seen that the friction coefficient of TC-0° sample stabilizes at 0.4–0.5 with different spacings and that of TC-45° and TC-90° samples stabilizes at 0.5–0.6 with different spacings. Meanwhile, the average friction coefficient of different samples in the stable stage (450–1800 s based on Fig. 5) is calculated and that is shown in Fig. 6. It is noted that the TC-0° sample exhibits the lowest friction coefficient compared with TC-45° and TC-90° samples and the TC-90° sample exhibits higher friction coefficient than TC-45° sample. Meanwhile, it is found that the groove spacing seems to have a potential effect on the friction coefficient, and the textured samples (TC-0°, TC-45°, and TC-90°) with the spacing of 400 μm exhibit the lowest friction coefficient compared with the smooth sample. The average friction coefficient of the TC-0°, TC-45°, and TC-90° samples is reduced by 40.99, 30.31, and 28.17% at the spacing of 400 μm compared with the smooth surface, respectively.

3.3 Wear volume of the balls

The wear volumes of the counter balls sliding against the smooth and textured AlCrN samples with different groove inclinations are calculated and are shown in Fig. 7. It can be seen that the groove inclination has a profound influence on the wear of the counter balls. The balls sliding against the TC-0° sample have the lowest wear volumes, and the wear volumes of the balls sliding against the TC-45° and TC-90° samples are larger than that sliding against the UTC sample. In addition, it can be seen that the wear volumes of balls sliding against the textured AlCrN samples with the spacing of 400 μm seem to be lower than that with the spacing of 300 and 500 μm.

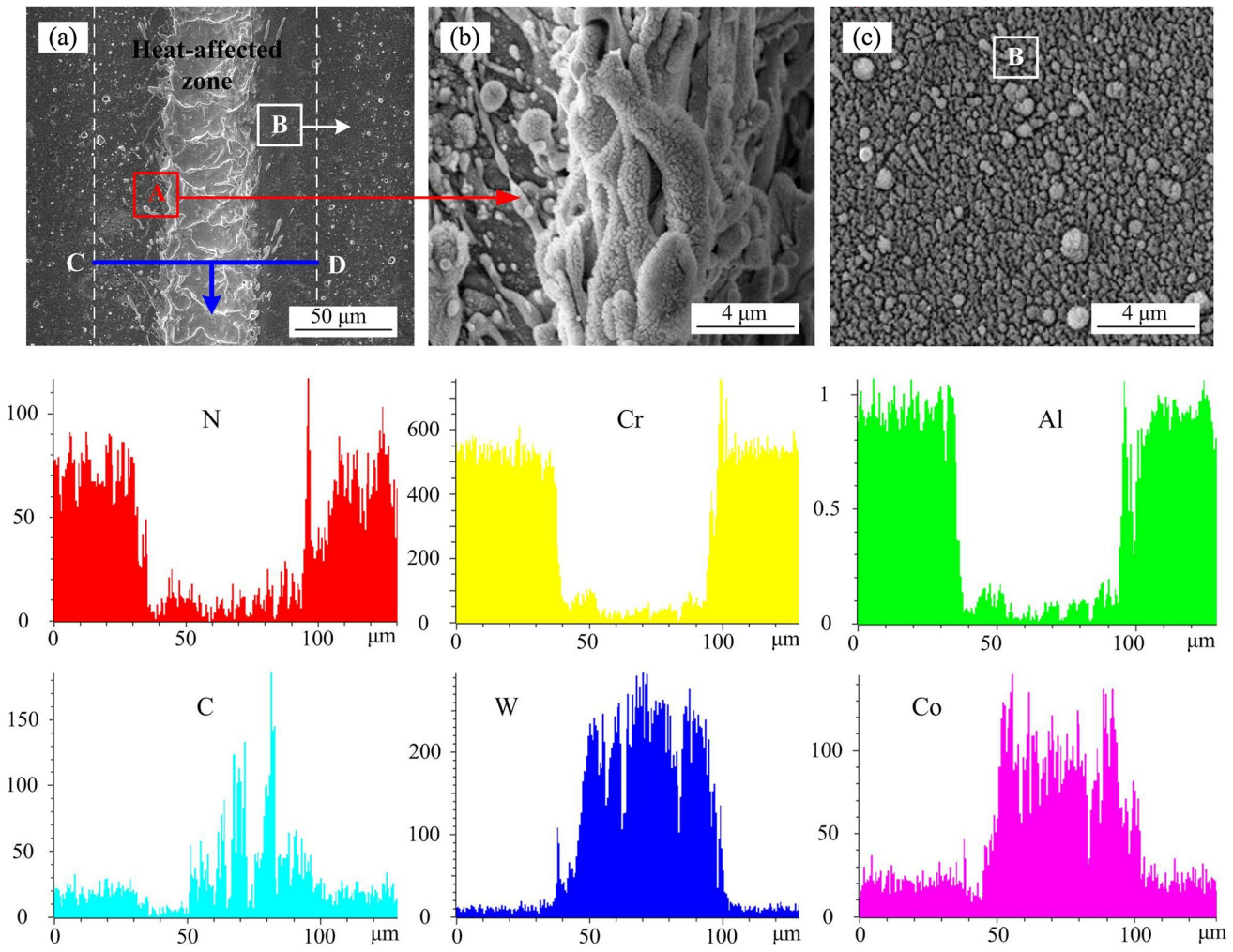

Fig. 4 SEM micrographs of the groove and EDX analyses of line CD

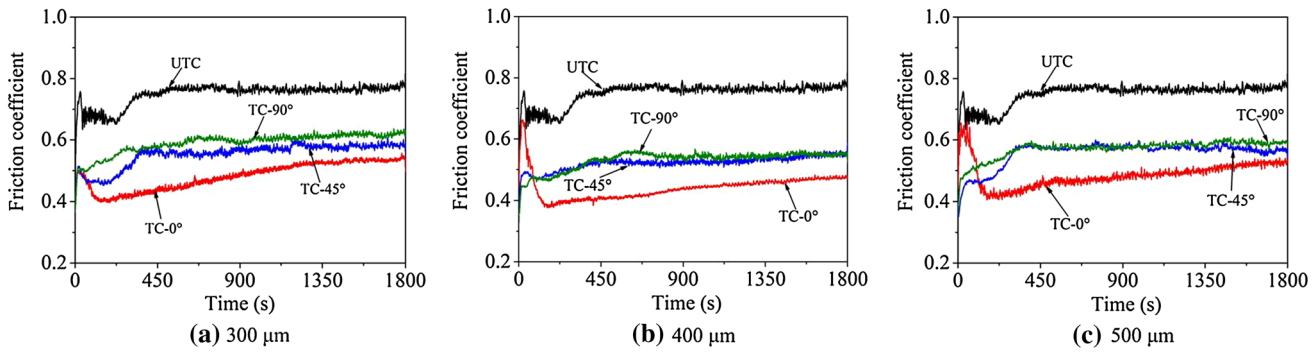

Fig. 5 Comparison of friction coefficient of the smooth and textured AlCrN samples with different groove inclinations at the different spacings

3.4 Worn morphologies

Figure 8 shows the worn morphologies of the smooth and textured AlCrN surfaces with different groove inclinations at spacing of 400 μm after 30 min dry friction. It can be seen that the wear scar of the UTC sample is different with that of the TC-0°, TC-45°, and TC-90° samples; severe surface damages occur on the UTC sample compared with the textured samples, and the groove inclination has an influence on the worn scars. The grooves on the wear scars of textured

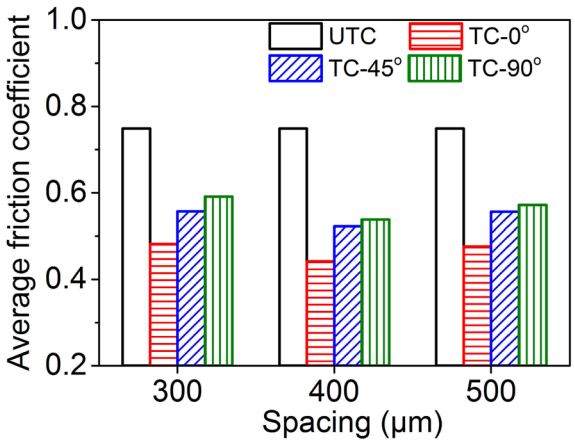

Fig. 6 Comparison of average friction coefficient of the smooth and textured AlCrN samples with different groove inclinations at the different spacings

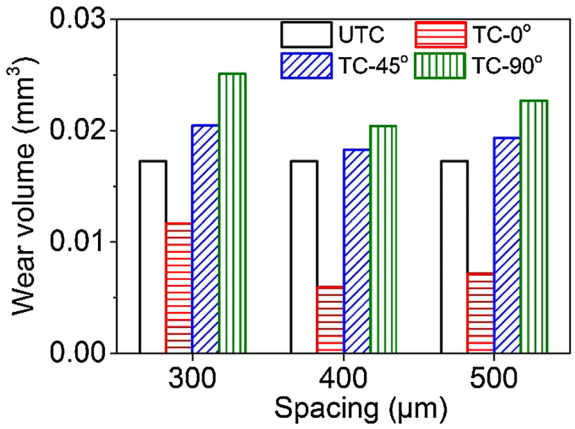

Fig. 7 Wear volumes of the balls sliding against the smooth and textured AlCrN samples with different groove inclinations at different spacings

samples are embedded with some debris. To better analyze the surface morphologies, the two-dimensional worn morphologies and profiles of the wear scars are detected and that are shown in Fig. 9. As shown in this figure, the wear width of TC-0° is smaller compared with the UTC sample, and the wear widths of TC-45° and TC-90° are larger compared with the UTC sample. Meanwhile, large amounts of wear debris are adhered to the worn surface, and the adhesion height of the UTC sample is the largest than that of the TC-0°, TC-45°, and TC-90° samples. In addition, as clearly seen in Fig. 9b′, some debris fills in the grooves.

To further assess the adhesions on the wear scars of the smooth and textured AlCrN surfaces with different groove inclinations, the SEM micrographs and EDX maps of the distribution of Fe element on the worn surfaces of UTC, TC-0°, TC-45°, and TC-90° samples after 30 min dry friction are shown in Fig. 10. As exhibited, large amounts of adhesions of Fe distribute on the worn surface of UTC sample; while for TC-0°, TC-45°, and TC-90° samples, the adhesions of Fe are mainly concentrated on the grooves. Comparison with TC-45° and TC-90° samples, few adhesions are distributed on the space surface between the grooves of TC-0° sample. To further investigate the differences of worn surfaces between smooth and textured samples, the enlarged SEM micrographs of the worn surfaces of UTC and TC-0° samples and the corresponding EDX analyses are shown in Fig. 11. It further reveals that more adhesions of Fe distribute on the worn surface of UTC sample compared with TC-0° sample confirmed by the EDX analyses of points A and C (see Fig. 11b, c, f, g). Meanwhile, the EDX analyses of points B and D show that the large amounts of Al, Cr, and N elements still exist on the worn surfaces.

Figure 12 illustrates the worn surfaces of the balls sliding against the smooth and textured AlCrN samples with different groove inclinations at spacing of 400 μm after 30 min dry friction. As can be seen in this figure, abrasive wear is the mainly wear mechanism of the ball surfaces, and the plows are gradually obvious with the decreasing groove inclination ranging from 90° to 0°.

4 Discussion

The friction and wear properties of the microtextures with different angles on AlCrN coatings under dry condition are investigated. Results show that the microtextures can improve the tribological properties of AlCrN coatings, and the angle between the groove inclination and sliding direction has a significant influence on the tribological behavior of the AlCrN sample sliding against AISI 1045 steel ball. Experimental results show that the TC-0° sample exhibits the lowest friction coefficient compared with TC-45° and TC-90°, see Figs. 5, 6, which indicates that the microtextured AlCrN sample with the grooves parallel to the sliding direction is the most effective in improving the tribological properties. It can be explained that the friction property is strongly related to the real contact area and the retarding force that is perpendicular to the groove inclination induced by the groove edges [29, 30]; the reduced contact area for textured samples is responsible for the low friction coefficient compared with the smooth sample. Comparisons of the textured AlCrN samples with different groove inclinations, the retarding force for textured samples reduces with the decreasing groove inclination [29], which results in the low friction coefficient for TC-0° sample. Meanwhile, it is noted that the wear volume of the counter ball sliding against the TC-0° sample is the smallest among the experiments, and the sliding against the TC-45° and TC-90° samples is larger compared with the UTC sample; the similar results

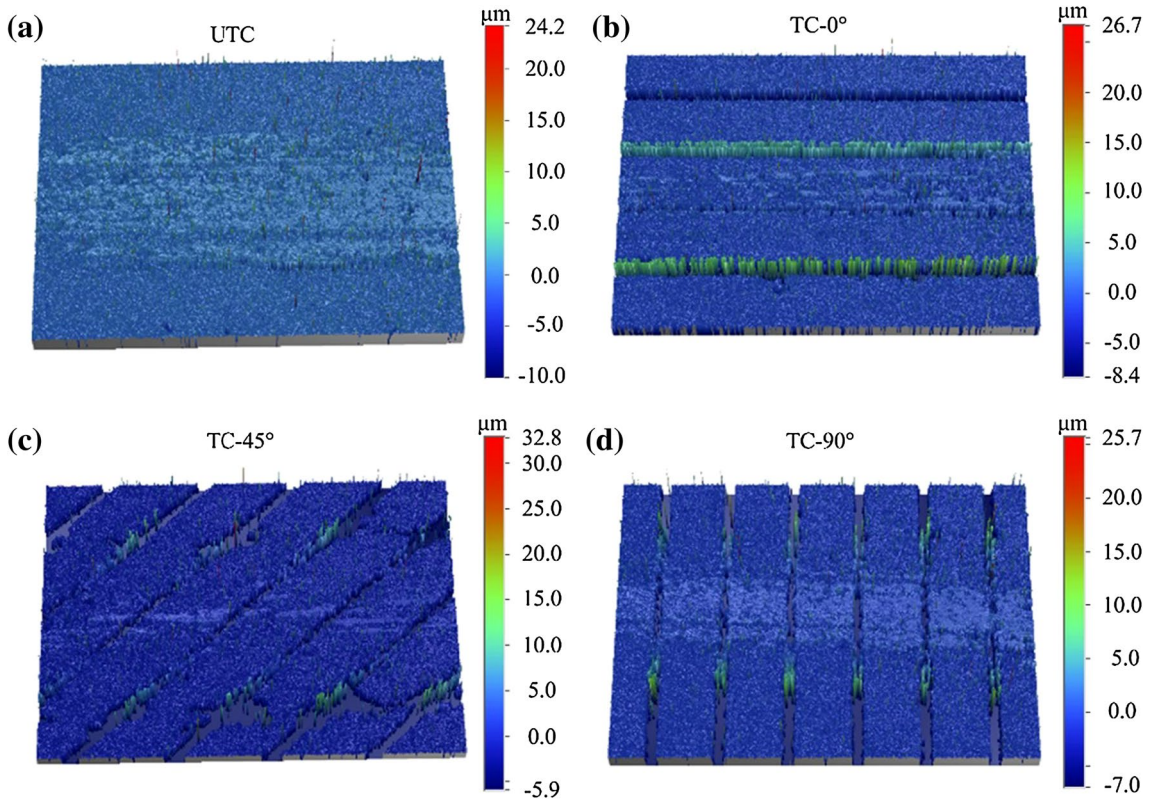

Fig. 8 Three-dimensional worn morphologies of the smooth and textured AlCrN surfaces with different groove inclinations at spacing of 400 μm after 30 min dry friction

are reported in literature [31, 32]. It can be explained that for TC-0° sample, the low friction at the interface results in a small wear volume of the ball, and for TC-45° and TC-90° samples, the large wear volume of the balls can be ascribed to the microcutting effect of the groove edges. On the other hand, the groove spacing seems to have a potential influence on the friction properties of the textured AlCrN surface, and with respect to this further investigates will be conducted next.

According to the experimental results, adhesion is the main wear form of AlCrN-coating surface that sliding against the AISI 1045 steel ball, which is attributed to the immense differentia in hardness between AlCrN coatings and the AISI 1045 hardened steel. The worn morphologies of the AlCrN samples demonstrate that the microtextures reduce the adhesions on the worn surface, and the grooves are filled with debris. The results indicate that the improvement of worn surface is attributed to the effect of entrapment of debris by the grooves, as shown in Figs. 8, 10, where large amounts of wear debris fill in the grooves. In this case, the grooves are as reservoirs of debris that leave free interfaces between the ball and textured AlCrN surface, and thus reduce the adhesions on the worn surface. While, the microgrooves will be replicated to the worn surface of the counter balls, and then leads to the generation of plows, especially for the TC-0° sample, as shown in Fig. 12b, b′. The existence of Al, Cr, and N elements on the enlarged worn surfaces of UTC and TC-0° samples confirmed by the EDX analyses of points A and D (Fig. 11) indicates that the AlCrN coatings are still retained after the friction and wear tests.

5 Conclusions

Microtextures with different inclinations are fabricated on the surface of AlCrN-coated samples using a nanosecond laser, and the friction and wear properties of the textured surface sliding against the AISI 1045 steel ball are investigated by reciprocating ball-on-disk friction tests under dry conditions. The main conclusions are summarized:

1. Microtextures induced by nanosecond laser are effective in reducing the friction coefficient of the AlCrN-coated sample sliding against the AISI 1045 steel, and the friction properties are quite sensitive to the groove inclination. The TC-0° sample exhibits the lowest friction coefficient compared with TC-45° and TC-90° samples, indicating that the grooves parallel to the sliding

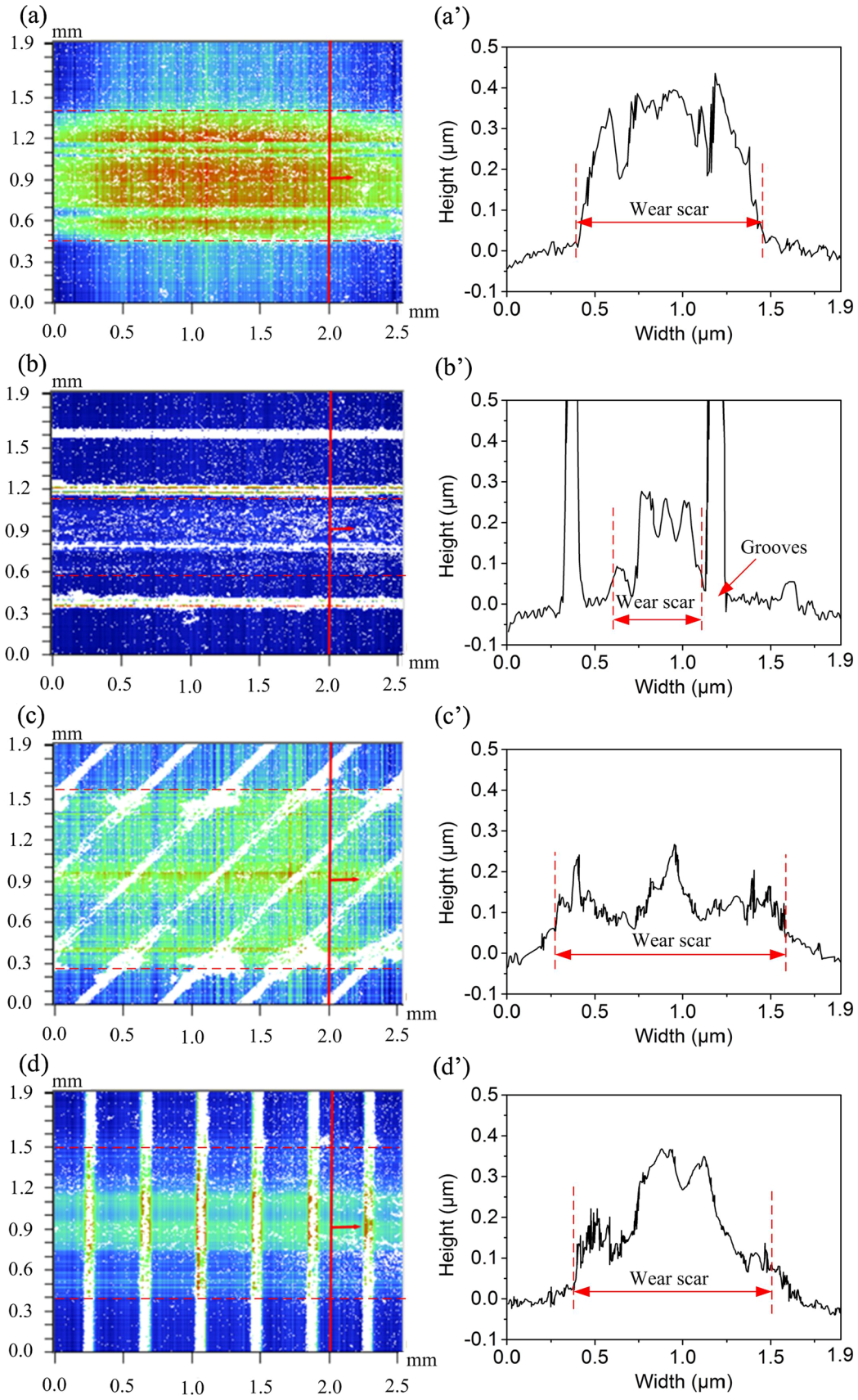
(a)
mm
1.9
1.5
1.2
0.9
0.6
0.3
0.0
0.0 0.5 1.0 1.5 2.0 2.5
mm
(a')
Height (μm)
0.5
0.4
0.3
0.2
0.1
0.0
-0.1
Wear scar
0.0 0.5 1.0 1.5 1.9
Width (μm)
(b)
mm
1.9
1.5
1.2
0.9
0.6
0.3
0.0
0.0 0.5 1.0 1.5 2.0 2.5
mm
(b')
Height (μm)
0.5
0.4
0.3
0.2
0.1
0.0
-0.1
Grooves
Wear scar
0.0 0.5 1.0 1.5 1.9
Width (μm)
(c)
mm
1.9
1.5
1.2
0.9
0.6
0.3
0.0
0.0 0.5 1.0 1.5 2.0 2.5
mm
(c')
Height (μm)
0.5
0.4
0.3
0.2
0.1
0.0
-0.1
Wear scar
0.0 0.5 1.0 1.5 1.9
Width (μm)
(d)
mm
1.9
1.5
1.2
0.9
0.6
0.3
0.0
0.0 0.5 1.0 1.5 2.0 2.5
mm
(d')
Height (μm)
0.5
0.4
0.3
0.2
0.1
0.0
-0.1
Wear scar
0.0 0.5 1.0 1.5 1.9
Width (μm)

◂**Fig. 9** Two-dimensional surface micrographs and profiles of the wear scars of the smooth and textured AlCrN surfaces with different groove inclinations at spacing of 400 μm after 30 min dry friction

direction are the most effective in improving the friction properties of the AlCrN surface.

2. The TC-0° sample reduces the wear volume of the counter ball compared with the UTC sample due to the reduced interface friction coefficient, while the TC-45° and TC-90° samples increase the wear volumes of the counter balls compared with the UTC sample, which may be ascribed to the stronger microcutting effect induced by the groove edges.
3. Adhesions are the main wear mechanism of AlCrN surface sliding against the AISI 1045 steel, and the microtextured samples (TC-0°, TC-45°, and TC-90°) can effectively reduce the adhesions. The TC-0° sample exhibits the smallest adhesions due to the effect of capturing debris by the grooves and the low friction coefficient at the interface.

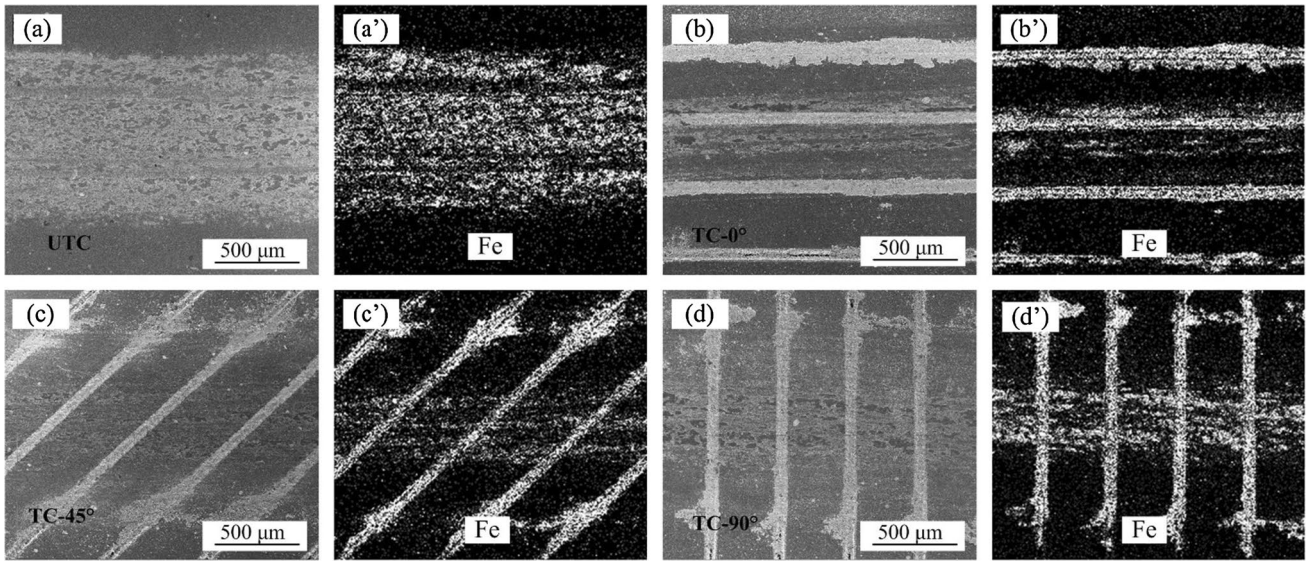

Fig. 10 SEM micrographs of the worn surfaces of UTC, TC-0°, TC-45°, and TC-90° samples and the corresponding EDX maps of the distribution of Fe element after 30 min dry friction

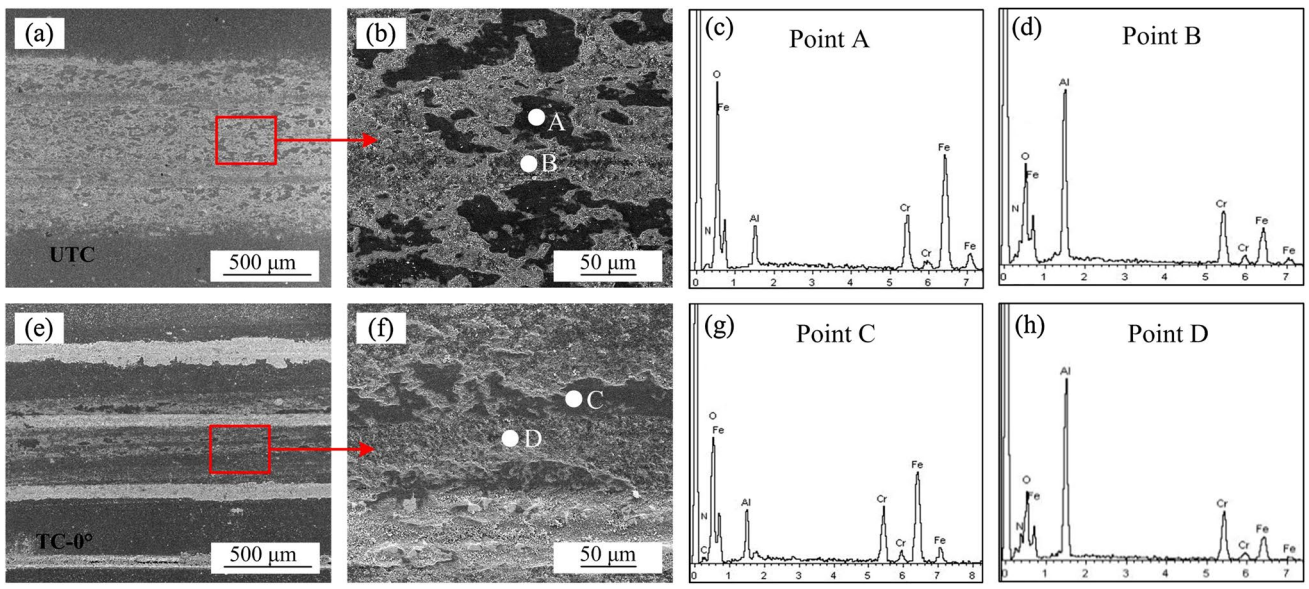

Fig. 11 SEM micrographs of the worn surfaces of UTC and TC-0° samples and the corresponding EDX analyses of points A to D after 30 min dry friction

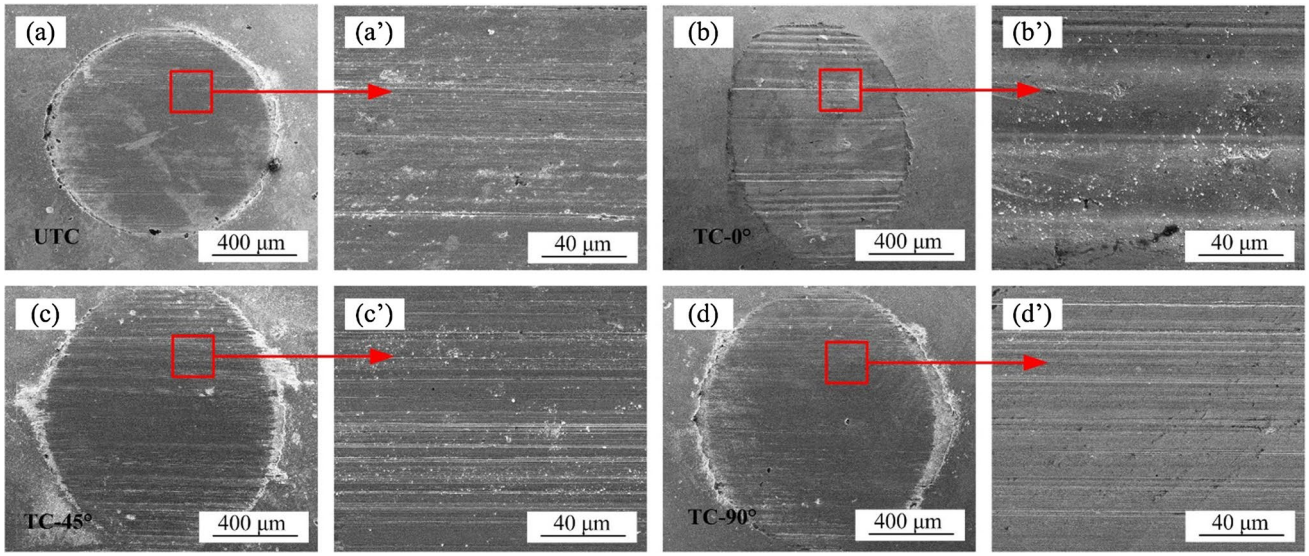

Fig. 12 SEM micrographs of the worn surfaces of the balls sliding against the smooth and textured AlCrN samples with different groove inclinations at spacing of 400 μm after 30 min dry friction

Acknowledgements This work is supported by the National Natural Science Foundation of China (51675311, 51405080), the Natural Science Foundation of Jiangsu Province (BK20170676), and the Development Plan of Science and Technology of Shandong Province (2017GGX30115).

References

1. S.C. Cha, A. Erdemir, *Coating Technology for Vehicle Applications* (Springer, Switzerland, 2015)
2. W. Kalss, A. Reiter, V. Derflinger, C. Gey, J.L. Endrino, Modern coatings in high performance cutting applications. Int. J. Refract. Met. Hard Mater. **24**(5), 399–404 (2006)
3. Y.J. Lin, A. Agrawal, Y. Fang, Wear progressions and tool life enhancement with AlCrN coated inserts in high-speed dry and wet steel lathing. Wear **264**(3), 226–234 (2008)
4. J.L. Endrino, G.S. Fox-Rabinovich, C. Gey, Hard AlTiN, AlCrN PVD coatings for machining of austenitic stainless steel. Surf. Coat. Technol. **200**(24), 6840–6845 (2006)
5. K.D. Zhang, J.X. Deng, J.L. Sun, C. Jiang, Y.Y. Liu, S. Chen, Effect of micro/nano-scale textures on anti-adhesive wear properties of WC/Co-based TiAlN coated tools in AISI 316 austenitic stainless steel cutting. Appl. Surf. Sci. **355**, 602–614 (2015)
6. T. Obikawa, A. Kamio, H. Takaoka, A. Osada, Micro-texture at the coated tool face for high performance cutting. Int. J. Mach. Tools Manuf. **51**, 966–972 (2011)
7. P.W. Shum, Z.F. Zhou, K.Y. Li, Friction and wear reduction of hard TiAlSiN coatings by an integrated approach of laser surface texturing and high-energy ion implantation. Surf. Coat. Technol. **259**, 136–140 (2014)
8. A.A. Voevodin, J.S. Zabinski, Laser surface texturing for adaptive solid lubrication. Wear **261**, 1285–1292 (2006)
9. G. Dumitru, V. Romano, Y. Gerbig, H. Haefke, Femtosecond laser processing of nitride-based thin films to improve their tribological performance. Appl. Phys. A **80**(2), 283–287 (2005)
10. M. Nakano, A. Korenaga, A. Korenaga, K. Miyake, T. Murakami, Y. Ando, H. Usami, S. Sasaki, Applying micro-texture to cast iron surfaces to reduce the friction coefficient under lubricated conditions. Tribol. Lett. **28**, 131–137 (2007)
11. I. Etsion, State of the art in laser surface texturing. J. Tribol. **127**(1), 248 (2005)
12. W. Grabon, P. Pawlus, S. Wos, W. Koszela, M. Wieczorowski, Effects of honed cylinder liner surface texture on tribological properties of piston ring-liner assembly in short time tests. Tribol. Int. **113**, 137–148 (2017)
13. L. Sabri, M.E.I. Mansori, Process variability in honing of cylinder liner with vitrified bonded diamond tools. Surf. Coat. Technol. **204**, 1046–1050 (2009)
14. Z. Wu, J.X. Deng, Y.Q. Xing, H.W. Cheng, J. Zhao, Effect of surface texturing on friction properties of WC/Co cemented carbide. Mater. Des. **41**, 142–149 (2012)
15. Y.Q. Xing, J.X. Deng, X.S. Wang, K. Ehmann, J. Cao, Experimental assessment of laser textured cutting tools in dry cutting of aluminum alloys. J. Manuf. Sci. Eng. **138**(7), 071006 (2016)
16. U. Pettersson, S. Jacobson, Friction and wear properties of micro textured DLC coated surfaces in boundary lubricated sliding. Tribol. Lett. **17**(3), 553–559 (2004)
17. H. Hata, T. Nakahara, H. Aoki, Measurement of friction in lightly load hydrodynamic sliders with striated roughness. In *Proceedings of the winter annual meeting of the American Society of Mechanical Engineers*, Chicago, Illinois, 1980, pp. 75–92
18. A. Rosenkranz, L. Reinert, C. Gachot, F. Mücklich, Alignment and wear debris effects between laser-patterned steel surfaces under dry sliding conditions. Wear **318**, 49–61 (2014)
19. Z. Wang, Y.-B. Li, F. Bai, C.-W. Wang, Q.-Z. Zhao, Angle-dependent lubricated tribological properties of stainless steel by femtosecond laser surface texturing. Opt. Laser Technol. **81**, 60–66 (2016)
20. S.H. Yuan, W. Huang, X.L. Wang, Orientation effects of micro-grooves on sliding surfaces. Tribol. Int. **44**, 1047–1054 (2011)
21. H.L. Costa, I.M. Hutchings, Hydrodynamic lubrication of textured steel surfaces under reciprocating sliding conditions. Tribol. Int. **40**, 1227–1238 (2007)

22. S. Mezghani, I. Demirci, H. Zahouani, M.E.I. Mansori, The effect of groove texture patterns on piston-ring pack friction. Precis. Eng. **36**(2), 210–217 (2012)
23. M.-S. Suh, Y.-H. Chae, S.-S. Kim, T. Hinoki, A. Kohyama, Effect of geometrical parameters in micro-grooved crosshatch pattern under lubricated sliding friction. Tribol. Int. **43**, 1508–1517 (2010)
24. A. Dunn, K.L. Wlodarczyk, J.V. Carstensen, E.B. Hansen, J. Gabzdyl, P.M. Harrison, J.D. Shepharda, D.P. Hand, Laser surface texturing for high friction contacts. Appl. Surf. Sci. **357**, 2313–2319 (2015)
25. Y.Q. Xing, J.X. Deng, Z. Wu, F.F. Wu, High friction and low wear properties of laser-textured ceramic surface under dry friction. Opt. Laser Technol. **93**, 24–32 (2017)
26. A. Dunn, J.V. Carstensen, K.L. Wlodarczyk, E.B. Hansen, J. Gabzdyl, P.M. Harrison, J.D. Shephard, D.P. Hand, Nanosecond laser texturing for high friction applications. Opt. Lasers Eng. **62**, 9–16 (2014)
27. Z. Wang, Q.Z. Zhao, C.W. Wang, Y. Zhang, Modulation of dry tribological property of stainless steel by femtosecond laser surface texturing. Appl. Phys. A **119**, 1155–1163 (2015)
28. Z. Wu, J.X. Deng, H. Zhan, Y.S. Lian, J. Zhao, Tribological behavior of textured cemented carbide filled with solid lubricants in dry sliding with titanium alloys. Wear **292**, 135–143 (2012)
29. Y.Q. Xing, J.X. Deng, X.T. Feng, S. Yu, Effect of laser surface texturing on Si_3N_4/TiC ceramic sliding against steel under dry friction. Mater. Des. **52**, 234–245 (2013)
30. V. Franzen, J. Witulski, A. Brosius, M. Trompeter, A.E. Tekkaya, Textured surfaces for deep drawing tools by rolling. Int. J. Mach. Tools Manuf. **50**, 969–976 (2010)
31. Y.Q. Xing, J.X. Deng, Z. Wu, H.W. Cheng, Effect of regular surface textures generated by laser on tribological behavior of Si_3N_4/TiC ceramic. Appl. Surf. Sci. **265**, 823–832 (2013)
32. A. Kovalchenko, O. Ajayi, A. Erdemir, G. Fenske, Friction and wear behavior of laser textured surface under lubricated initial point contact. Wear **271**(9), 1719–1725 (2011)